American Journal of Applied Sciences and Engineering | *ISSN 2766-7596*
Published by AIR JOURNALS | *https://airjournal.org/ajase*
12011 WestBrae Pkwy, Houston, TX 77031, United States
airjournals@gmail.com; enquiry@airjournal.org

Research article

Characterization and Development of a Simulink Model of 330kv Nigeria Power Transmission Network

Ude Kingsley Okechukwu[1], and Prof. G. N. Onoh[2]

[1,2]Electrical and Electronics Engineering Department, Enugu State University of Science and Technology, Nigeria

Accepted: December 8th, 2022	Published: December 12th, 2022

Citations - APA

Okechukwu, U. K. & Onoh, G. N. (2022). Characterization and Development of a Simulink Model of 330kv Nigeria Power Transmission Network. *American Journal of Applied Sciences and Engineering, 3(6), 38-50. DOI:* https://doi.org/10.5281/zenodo.7433486

ABSTRACT

There is a gross shortage of electrical energy in Nigeria. The demand for electric power is way too high than the supply and the Nigerian state seems not to be able to install new transmission facilities to mitigate the shortage. The transmission facilities especially have been overstretched in a bid to wheel more power to the distribution systems. It has therefore become imperative to devise a means of improving the performance of the existing transmission network to ensure that it continues to operate optimally pending when it will be expanded. Against this backdrop, this study characterizes the Nigeria transmission network to ascertain the present operating condition of the system with a view to enhancing it. This is inspired by the fact that the network available transfer capacity (ATC), voltage profile, and loss reduction can be improved if the network is properly characterized with a view to enhancing these indices. The case study network was modeled on Simulink/PSAT and Newton Raphson power flow (NRPF) and continuation power flow (CPF) was carried out on the modeled network with the help of MATLAB/PSAT. From the results obtained, the network ATC was determined with a view to improving it; likewise, the voltage profiles and the total power loss. Findings in this research work showed that the computed ATC of the test network before compensation was found to be 8.94pu. Also, with help of load flow studies, five buses were found to be weak (with a voltage profile less than 0.95pu) while the total network real power loss before compensation was found to be 0.5182pu.

Keywords: *Simulink Model of 330kv; Nigeria Power Transmission Network; Characterization and Development; Power Flow*

Vol. 3, No. 6 | 2022 | pp. 38-50 | *DOI: https://doi.org/10.5281/zenodo.7433486*

Introduction

Electricity has a major impact on every aspect of our socioeconomic life. It plays a vital role in the economic, social, and political development of any nation (Rachmawatie, 2019). In our present world today, electricity is the most widely used and desirable form of energy. According to Mohammad et al (2020), there is a causal relationship between an increase in a country's population and the demand for electricity. However, it is unfortunate that Power transmission capacity has not kept pace with consumer demand for power. One way to meet this demand is by building new power generation stations and transmission lines. However, as observed by Ahmad et al. (2014), the construction of new transmission systems is hindered by many factors such as ecological considerations, financial difficulties, and unavailability of space in overpopulated areas. Against this backdrop, many developing countries such as Nigeria have resorted to improving the performance of the existing power systems such as the transmission network. Enhancing the performance of the existing system brings along many advantages that cut across economical and technical gains. Some of the parameters that can be improved on an existing transmission network include the available transfer capacity (ATC), voltage profile, and reduction of total power loss in the network.

To achieve this enhancement, it is first and foremost required that the present condition of the network be ascertained to determine the most suitable parameters to improve to achieve the optimum performance of the system. This feat is achieved through the characterization of the network. Thus, the study focuses on the characterization of the Nigerian 47-bus transmission network to determine how best to improve the network ATC, and voltage profile and to reduce the total power loss.

Available transfer capability (ATC) is a measure of the transfer capability remaining in the physical transmission network for further commercial activity over and above the already committed uses (NERC Report, June 1996). ATC of the test system is a measure of how much power can be delivered from the source area (slack bus) to the sink area (load bus) in the bus system. Since it considers the two limitations between line and voltage limits, hence the power of each bus and the line voltage should be taken into consideration. Available Transfer capability plays an important role in the electricity market since due to some constraints, the transmission lines are utilized significantly below their physical limits. Therefore, by increasing the transfer capability, the overall efficiency will increase and more energy trading can take place between the competing regions operating (Hojabri, et al., 2011). The power system needs to be ensured that the power transfers are within the system transfer capability.

Power flow on the elements of the transaction interface changes depending on some factors such as generation dispatches, the level of customer demand, network topology, and other transactions in the system. Therefore, the ATC transmission network becomes an important function of all these variables. In fact, adequate available transfer capability (ATC) is needed to ensure all economic transactions. Sufficient ATC should be guaranteed to support free market trading and maintain an economical and secure operation over a wide range of system conditions. The transmission system must be very flexible, every second of every day, to meet the demands of the country's growing need for electricity that must be reliable and affordable (Elias and Sarwary, 2017). These concerns have motivated the development of strategies to increase the ATC of the existing transmission network.

Literature Review
Principles of Newton-Raphson Method

The Newton-Raphson method is based on Taylor's series and partial derivatives. The Newton-Raphson method is recent, needs less number of iterations to reach convergence, takes less computer time, and hence computation cost is less and the convergence is certain. The N-R method is more accurate and less sensitive to factors like slack bus selection, regulating transformers, etc. and the number of iterations in this technique is almost independent of the system size.

The disadvantage of this method is the difficult solution technique, more calculations involved in each iteration resulting in large computer time per iteration, and the large requirement of computer memory. This last drawback has been overcome through a compact storage scheme.

Convergence can be considerably speeded up by performing the first iteration through the G-S method and using the value of voltages so obtained for starting the N-R iteration. These voltages are used to compute active power at every bus except the swing bus and also reactive power Q where reactive power is specified. The process of iteration is continued till the difference in the specified and calculated values of P, Q and V are within the given permissible limit (Gupta, 2014).

The Principle of Continuation Power Flow
This analysis method makes use of an iterative process that involves two steps: the predictor and corrector steps. For a specified pattern of load increase, a tangent predictor is used to estimate solution (B) from an initial known solution (A). By assuming a fixed system load and using a conventional load flow analysis, the corrector step is used to determine the exact solution C. Based on a new tangent predictor; the voltages for a further increase in load are then predicted. Convergence will fail if the next estimated Load (D) is beyond the maximum load on the exact solution. To resolve this, a corrector step with a fixed voltage at the monitored bus is applied to locate the exact solution. To determine the exact solution for approaching the voltage stability limit, there is a need for the load increase to be gradually reduced during successive predictor steps (Fosso, 2016).

Review of Related Literature

Natália et al. (2018) observed that in the deregulated power system, competition arises in generation and distribution but the transmission corridor remains the same for transferring power. Every operator wants to maximize profit and as such the number of transactions increases. This according to their observation may cause congestion in the transmission network. To avoid this, they proposed that every operator should know the value of available transfer capability (ATC) before every transaction. However, the determination of ATC is a complex task that has to be done at periodic intervals for each source and sink pair. Though there are many methods available to assess ATC, they suggested that the most accurate method is repeated power flow using Newton Raphson (RPFNR). Thus, they applied the RPFNR approach on both 3-bus and 14-bus networks by modeling and simulation using Power World Simulator (PWS). ATC between nodes and areas for both networks was determined. The error difference between ATC gotten from both procedures was negligible. A 14-bus system was further modeled, and ATC between nodes and areas was determined.

Similarly, Chandrasekar et al. (2011) investigated repeated power flow using the Broyden-Shamanski method. This method eradicates the drawback of the Newton-Raphson method (which requires very high computational time). The proposed technique was tested with a WSSC 9-bus, New England 39-bus and IEEE 144-bus tested system and the results were compared with the conventional RPF using Newton Raphson. At the end of the work, the result showed that the computational time is far less than the conventional Newton-Raphson method while maintaining accuracy.

American Journal of Applied Sciences and Engineering | AJASE
Vol. 3, No. 6 | 2022 | pp. 38-50 | *DOI: https://doi.org/10.5281/zenodo.7433486*

Naresk and Prashant (2012) made a proposal on ATC calculation using the DC power flow model for both single and multiple transactions. ATC is calculated for both intact and contingency cases. Two types of contingencies were considered. Implementation of a novel method known as Hybridized Continuous Repeated Power Flow (HCR-PF) to compute inter-area ATC was carried out by Ahmad (2014) and he formulated a method based on computed ATC in evaluating the transmission efficiency by measuring the transfer efficiency of the transmission system in order to obtain ATC. The result showed that HCR-PF is a good alternative for ATC computation after due validation using the IEEE 30-bus test network.

Methodology

Development of a Simulink Model for the Test Network

It is very imperative to accurately model the network. The procedure applied to achieve this objective is presented thus: the power system toolbox (PSAT) was used to create a new workspace in the Simulink environment. The needed component blocks (generators, transmission lines, buses, load, etc.) were then imported into the virgin workspace.

Consequently, they are connected accordingly to yield the 47-bus network. Finally, the components are set to the exact values specified in bus data and line data. Figure 1 shows the developed Simulink model of the test network.

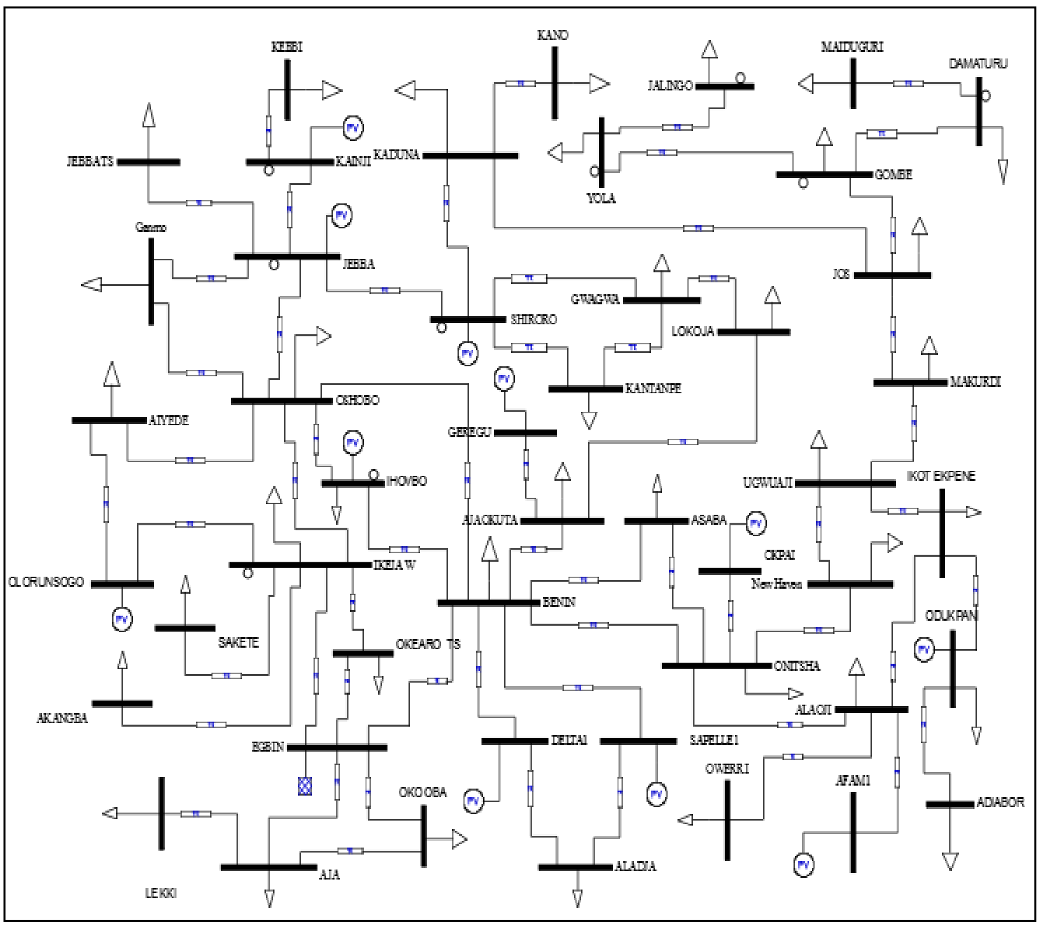

Figure 1: Developed Simulink model of the test network

Newton-Raphson Load Flow Representation Using Polar Coordinates

Having developed a model of the test network, it is ideal to carry out power flow studies on the network to ascertain the electrical conditions of the network. This study adopts the Newton Raphson method of power flow studies owing to its peculiar suitability in this case. Thus, the Newton-Raphson load flow representation in polar coordinates has been formulated as presented by Gupta (2014);

for any ith bus, we have

$\boldsymbol{V_i} = V_i e^{j\delta i}$, then $V_i^* = V_i e^{-j\delta i}$

and $V_k = V_k e^{j\delta k}$

and $Y_{ik} = Y_{ik} e^{-j\theta ik}$ (1)

where δ is the phase angle of the bus voltages and θ_{ik} is an admittance angle

For any ith bus

$S^* = P_i - jQ_i = V_i^* \sum_{k=1}^{n} Y_{ik} V_k; i = 1,2,3,..n$ (2)

Substituting the values of V_i^*, V_k *and* Y_{ik} from Equation (1) in equation (2) we have

$p_i - jQ_i = \sum_{k=1}^{n} V_i V_k Y_{ik} e^{-j(\theta_{ik}+\delta_i-\delta_k)}$ (3)

Thus$P_i = \text{Real } V_i^* \sum_{k=1}^{n} Y_{ik} V_{ik} = \sum_{k=1}^{n} V_i V_k Y_{ik} \cos(\theta_{ik} + \delta_i - \delta_i)$

$= V_i V_i Y_{ii} \cos\theta_{ii} + \sum_{\substack{k=1 \\ k\neq i}}^{n} V_i V_k Y_{ik} \cos(\theta_{ik} + \delta_i - \delta_k)$ (4)

and $Q_i = I\text{maginary } \boldsymbol{V_i^* \sum_{k=1}^{n} Y_{ik} Y_k}$

$$= \sum_{k=1}^{n} V_i V_k Y_k \sin(\theta_{ik} + \delta_i - \delta_k)$$

$= \boldsymbol{V_i V_i Y_{ii}} sin\theta_{ii} + \sum_{\substack{k=1 \\ k\neq i}}^{n} V_i V_k Y_{ik} \sin(\theta_{ik} + \delta_i - \delta_k)$ (5)

for $i = 2,3,3,4, \ldots n$ because bus 1 is slack bus

Now the linear equation in polar form becomes

$$\begin{bmatrix} \Delta\boldsymbol{P} \\ \Delta\boldsymbol{Q} \end{bmatrix} = \begin{bmatrix} J_1 & J_2 \\ J_3 & J_4 \end{bmatrix} \begin{bmatrix} \Delta\boldsymbol{\delta} \\ \Delta\boldsymbol{V} \end{bmatrix} \quad (6)$$

where J_1, J_2, J_3 *and* J_4 are the elements of Jacobian matrix and can be determined from power equations (5) and (6) as follows:

The off-diagonal and diagonal elements of $J_1$are

$\frac{\partial P_i}{\partial \delta_k} = V_i V_k Y_{ik} \sin(\theta_{ik} + \delta_i + \delta_k)$ for $k \neq i$ (7)

and

$\frac{\partial P_i}{\partial \delta_i} = -\sum_{\substack{k=1 \\ k\neq i}}^{n} V_i V_k Y_{ik} \sin(\theta_{ik} + \delta_i - \delta_k)$ (8)

The off-diagonal and diagonal elements of J_2 are

$\frac{\partial P_i}{\partial V_k} = V_i Y_{ik} \cos(\theta_{ik} + \delta_i - \delta_k)\, fork \neq i$ (9)

And$\frac{\partial P_i}{\partial V_i}$ $2V_i Y_{ii} cos\theta_{ii} + \sum_{\substack{k=1 \\ k\neq 1}}^{n} V_k Y_{ik} \cos(\theta_{ik} + \delta_i - \delta_k)$ (10)

The off-diagonal elements of $J_3$are

$\frac{\partial Q_i}{\partial \delta_k} = -V_i V_k Y_{ik} cos(\theta_{ik} + \delta_i - \delta_k)$ (11)

and $\frac{\partial Q_i}{\partial \delta_i} = \sum_{\substack{k=1 \\ k\neq i}}^{n} V_i V_k Y_{ik} \cos(\theta_{ik} + \delta_i - \delta_k)$ (12)

The off-diagonal and diagonal elements of $J_4$are

$\frac{\partial Q_i}{\partial V_k} V_i Y_{ik} \sin(\theta_{ik} + \delta_i - \delta_k)\, fork \neq i$ (13)

and $\frac{\partial Q_i}{\partial V_i}\ 2V_iY_{ik}sin\theta_{ii} + \sum_{\substack{k=1 \\ k\neq i}}^{n} V_kY_{ik}\sin\left(\theta_{ik} + \delta_i - \delta_k\right)$ (14)

PSAT based Load Flow Study on the Test Network

The PSAT environment was first launched in Matlab. The bus and line data of the test network was then extracted and loaded into the PSAT environment. The bus data contains the name and code number of each of the fifty buses in the test network. The slack bus is coded 1, load buses (PQ) are coded 2, and generator buses (PV) are coded 3. There is one slack bus, eleven generator buses, and thirty-eight load buses. Egbin bus was chosen as the slack bus for having the highest magnitude of real power amongst the generator buses. The bus data presented in appendix A1 tabulates the bus names, their codes, real and reactive power generated by the generator buses, and real and reactive power load of the load buses. Line data contains the key line parameters of all the lines in the network. There are fifty-eight (58) lines in the network. The line data presented in appendix A2 tabulates the line numbers against their respective resistance and reactance values in pu. Bus and Line data were measured from the control room of the network under study. The Newton-Raphson Load flow algorithm option is selected. PSAT accepts the line and bus data and converts it to a usable format. On pushing the Run load flow button, PSAT uses the Newton Raphson load flow algorithm to perform load flow on the test network. After running the load flow, a tabulated result of the load flow is obtained from the static report. The load flow result on the test network is shown in Tables 1 and 2. Table 1 presents the 47 buses and their corresponding voltage magnitude (in pu), voltage angle (in rad), and change in real and power generated (in pu). Table 2 presents the network lines and their corresponding line flows (in pu) and line losses (in pu).

Performance of Continuation Load Flow in PSAT

The PSAT environment was first launched in Matlab. The bus and line data of the test network were then loaded into the PSAT environment. PSAT accepts the line and bus data and converts it to a usable format. On pushing the Run Continuation load flow button, PSAT uses the continuation load flow algorithm to perform continuation load flow on the test network. After running the continuation load flow, a tabulated result of the study is obtained from the static report. Continuation Load flow results on the test network was shown in Table 3. Table 3a presents the 47 buses and their corresponding voltage magnitude (in pu), voltage angle (in rad) and change in real and power generated (in pu). The buses and their corresponding voltage magnitudes are extracted from Table 3. The voltage magnitudes are then ranked from smallest to biggest. The weakest buses can then be identified based on the magnitude of their voltage magnitude such that the smaller the voltage magnitude the weaker the bus. In this method, the bus with the smallest voltage magnitude after the continuation load flow.

Continuation power flow overcomes the shortcoming of the conventional load flow methods. Conventional load flow techniques become singular at the nose point (point of voltage collapse). As a result, conventional load flow techniques are unable to compute load flow at the critical point (collapse point). Continuation load flow is able to produce load flow results at the collapse point when the network has been loaded (stressed) to its capacity limit. The load flow results obtained at the point of voltage collapse reveal the weakest buses of the network as their voltage profile will be most depleted at maximum loading. Voltage profiles of the test network are ranked from smallest to largest after the continuation load flow. Network buses with voltage profiles below 0.95pu are first identified as weak buses; where appropriate techniques can be deployed to enhance the network.

Grouping Selected buses into Source and Sink areas for ATC computation

In the procedure adopted in this research, some selected buses need to be grouped into two areas: source area and Sink area. The source area was made up of generator buses while the sink area was made up of load buses. Four generator buses: Kainji, Jebba, Shiroro and Ihovbo are identified as generators in the sources area. Similarly, Yola, Damaturu, Jalingo and Gombe are identified as loads in the sink area. A section of the test network showing the source (X) and sink (Y) areas with supply and demand supply bid blocks connected to the appropriate buses is shown in Figure 2.

American Journal of Applied Sciences and Engineering | AJASE
Vol. 3, No. 6 | 2022 | pp. 38-50 | DOI: https://doi.org/10.5281/zenodo.7433486

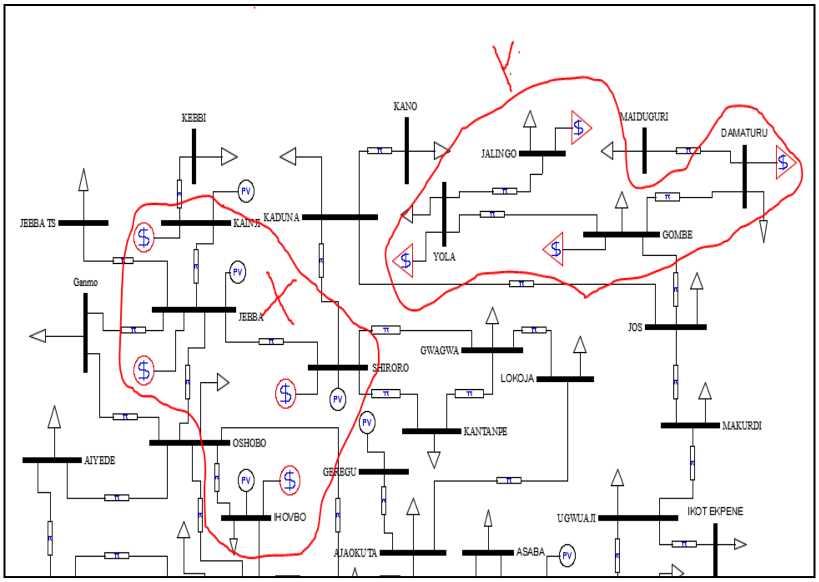

Figure 2: Section of the test network showing the source (X) and sink (Y) areas with supply and demand supply bid blocks connected to the appropriate buses

Newton Raphson conventional load flow is then performed on the test network to determine the real power loads on the buses of the sink area by (P_L^{io}). Transfer direction is then specified by connecting power supply bid block at all generator buses in source area and connecting power demand bid block at all load buses in sink area.

Computation of ATC of Network under Study

From the result obtained from load flow and continuation load flow on the network under study, real power loading at maximum loading are obtained for all the four load buses in the sink area ($P_L^i(\lambda_{max})$). ATC for the test network can be computed with equation 3.30 as proposed in Sadiq et al (2014).

$$ATC = \sum_{i \in sink} P_L^i(\lambda_{max}) - \sum_{i \in sink} P_L^{io} \tag{15}$$

The result of the load flow performed shows that the real power load for the four buses is given as; Yola (1pu), Gombe (1.6pu), Damaturu (1pu) and Jalingo (1pu). This gives a total of **4.6pu**. The real power load obtained for the four buses after continuation power flow are: Yola (3.38563pu), Gombe (3.98563pu), Damaturu (3.38563pu) and Jalingo (3.38563pu). This gives a total of **13.54pu**

Results and Discussion

Table 1: Voltage magnitude and angle, active and reactive power at buses after load flow

Bus	*V (pu)*	*phase (rad)*	*P gen (pu)*	*Q gen (pu)*	*P load (pu)*	*Q load (pu)*
ALAOJI	0.99774	-0.10303	0	0	3	-0.69
SAPELLE	1	-0.04478	4	-5.36141	0	0
AKANGBA	0.99512	-0.01606	0	0	2.04	0.95
LEKKI	1.00382	-0.01105	0	0	1.2	0.62
SAKETE	0.99039	-0.03045	0	0	2.04	0.95
AJA	1.00167	-0.00156	0	0	1.2	0.62
JEBBA	1	-0.02637	2.78	0.59784	0	0
KADUNA	0.97005	-0.11781	0	0	2	0.97

Vol. 3, No. 6 | 2022 | pp. 38-50 | DOI: https://doi.org/10.5281/zenodo.7433486

New Haven	0.99376	-0.09566	0	0	1.13	0.56
OKEARO TS	0.99724	-0.00923	0	0	2.04	0.95
SHIRORO	1	-0.07242	2	6.071	0	0
UGWUAJI	0.98481	-0.11271	0	0	1.6	0.95
ADIABOR	0.99825	-0.11346	0	0	1.82	0.67
AFAM	1	-0.09758	4.5	-2.54152	0	0
AIYEDE	0.99641	-0.02798	0	0	1.39	0.69
AJAOKUTA	1.00285	-0.05126	0	0	0.64	0.323
ALADJA	0.99979	-0.04764	0	0	1.82	0.67
ASABA	1.01252	-0.06247	0	0	0.15	0.076
BENIN	1.006	-0.05012	0	0	1.57	0.8
DAMATURU	0.89612	-0.19033	0	0	1	0.4
DELTA	1	-0.0467	2.5	-3.21335	0	0
EGBIN	1	0	25.04821	-5.51645	0	0
GEREGU	1	-0.04508	2	-1.17521	0	0
GOMBE	0.89641	-0.18913	0	0	1.6	0.95
GWAGWA	0.99999	-0.07123	0	0	2.03	1.02
GANMO	0.99472	-0.0334	0	0	1.39	0.69
IHOVBO	1	-0.03304	2	-5.38415	0.15	0.076
IKEJA W	0.99573	-0.01507	0	0	4.29	2.48
IKOT EKPENE	0.99556	-0.10769	0	0	1.82	0.67
JALINGO	0.88258	-0.19778	0	0	1	0.3
JEBBA TS	0.99973	-0.02679	0	0	0.15	0.076
JOS	0.95042	-0.1416	0	0	2.5	1.25
KAINJI	1	-0.01502	5.78	0.02132	0	0
KANO	0.96249	-0.12991	0	0	2	0.97
KANTANPE	0.99872	-0.07208	0	0	2.03	1.02
KEBBI	0.99846	-0.01841	0	0	1.2	0.4
LOKOJA	1.0019	-0.06148	0	0	0.15	0.076
MAIDUGURI	0.8933	-0.19755	0	0	1	0.3
MAKURDI	0.96322	-0.13168	0	0	1.8	0.65
ODUKPANI	1	-0.11233	2.5	1.25492	1.82	0.67
OKO OBA	1.00029	-0.00303	0	0	1.82	0.67
OKPAI	1	-0.07028	2.5	-1.29942	0	0
OLORUNSOGO	1	-0.01229	2.5	-0.28509	0	0
ONITSHA	1.00307	-0.07795	0	0	1.15	0.42
OSHOBO	0.99601	-0.03037	0	0	2.01	1.37
OWERRI	0.99243	-0.11836	0	0	2.04	0.95
YOLA	0.88392	-0.19415	0	0	1	4

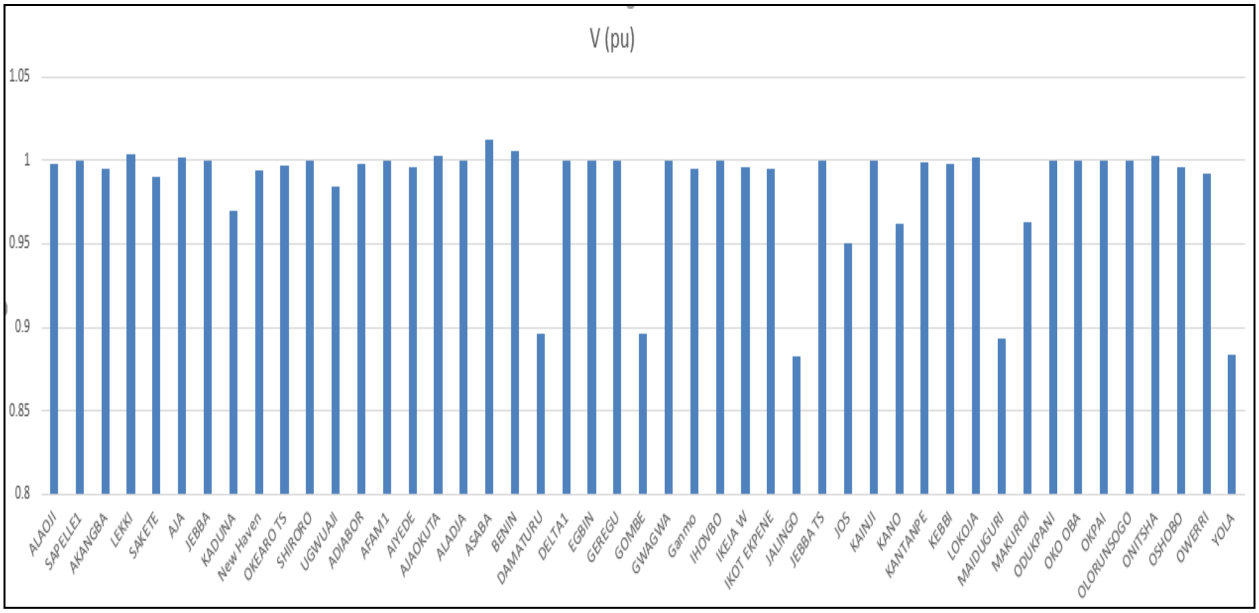

Figure 3: Bar Chart showing voltage magnitude of Test network buses after Load Flow.

Table 2: Load flow Result Showing Active and Reactive Power Flow in the Lines

From Bus	*To Bus*	*Line*	*P Flow (pu)*	*Q Flow (pu)*	*P Loss (pu)*	*Q Loss (pu)*
YOLA	GOMBE	1	-2.00042	-4.30409	0.00634	0.07093
EGBIN	AJA	2	2.78794	-3.19113	0.00032	0.0097
KADUNA	SHIRORO	3	-7.98708	-4.72989	0.05694	-1.27728
JEBBA	SHIRORO	4	6.13654	-0.57663	0.03305	0.28188
JOS	KADUNA	5	-3.96588	-2.60853	0.01746	0.14942
Ganmo	OSHOBO	6	-0.40723	-0.11981	0.00016	0.00139
IHOVBO	BENIN	7	2.13355	-6.0166	0.00497	-10.01761
UGWUAJI	New Haven	8	-5.15247	-1.80369	0.01506	0.10478
IKEJA W	AKANGBA	9	2.04031	0.95261	0.00031	0.00261
KANO	KADUNA	10	-2	-0.97	0.00373	0.03195
OSHOBO	BENIN	11	2.41163	-1.56034	0.0074	0.06346
MAKURDI	UGWUAJI	12	-6.02329	-5.18315	0.03335	0.23208
SHIRORO	KANTANPE	13	0.69747	0.92682	0.00121	0.00094
KEBBI	KAINJI	14	-1.2	-0.4	0.00048	0.00469
SHIRORO	GWAGWA	15	-0.638	0.83304	0.00099	0.00077
KANTANPE	GWAGWA	16	-1.33374	-0.09412	0.00161	0.00125
GOMBE	JOS	17	-5.60802	-5.20027	0.06915	0.58962
JEBBA TS	JEBBA	18	-0.15	-0.076	0.00001	0.00008
AIYEDE	OLORUNSOGO	19	-2.07392	-0.72693	0.0039	-1.00288
OSHOBO	IHOVBO	20	0.2839	-0.55347	0.00035	0.00298
OLORUNSOGO	IKEJA W	21	0.42218	-0.00915	0.00039	-1.03222
ALAOJI	AFAM1	22	-4.47596	2.56022	0.02404	0.0187
IKEJA W	EGBIN	23	-8.88438	-1.26971	0.01787	0.13973
IKEJA W	OKEARO TS	24	-3.42249	-0.42469	0.00264	0.02063

Vol. 3, No. 6 | 2022 | pp. 38-50 | DOI: https://doi.org/10.5281/zenodo.7433486

ALAOJI	**ONITSHA**	25	-6.04724	-3.11496	0.01812	-5.12944
OKEARO TS	**EGBIN**	26	-5.46513	-1.39533	0.00678	-0.98414
SAKETE	**IKEJA W**	27	-2.04	-0.95	0.00395	-0.99174
LEKKI	**AJA**	28	-1.2	-0.62	0.00143	-2.07915
ONITSHA	**New Haven**	29	6.31142	2.60375	0.0139	0.13528
OKO OBA	**EGBIN**	30	-1.43393	2.25771	0.00643	0.005
GWAGWA	**LOKOJA**	31	-4.00434	-0.2831	0.00467	0.03964
OKPAI	**ONITSHA**	32	2.5	-1.29942	0.00238	0.02318
AJAOKUTA	**LOKOJA**	33	4.16402	-0.60377	0.005	-1.00252
JOS	**MAKURDI**	34	-4.2113	-4.43137	0.012	0.10178
AJAOKUTA	**BENIN**	35	-2.80563	-0.91016	0.00779	0.00606
OWERRI	**ALAOJI**	36	-2.04	-0.95	0.00393	-0.99609
YOLA	**JALINGO**	37	1.00042	0.30409	0.00042	0.00409
DAMATURU	**MAIDUGURI**	38	1.00096	0.30818	0.00096	0.00818
GEREGU	**AJAOKUTA**	39	2	-1.17521	0.00161	0.01571
OKO OBA	**AJA**	40	-0.38607	-2.92771	0.00011	-5.28939
SAPELLE1	**ALADJA**	41	0.74682	-0.63062	0.00026	-1.19262
BENIN	**DELTA1**	42	-1.42356	3.34721	0.00288	0.02484
BENIN	**ONITSHA**	43	6.75019	0.00757	0.02206	0.1873
KAINJI	**JEBBA**	44	4.57952	-0.38337	0.00465	0.05195
BENIN	**SAPELLE1**	45	-3.24725	4.77661	0.00593	0.04582
DELTA1	**ALADJA**	46	1.07357	0.10903	0.00013	0.00102
DAMATURU	**GOMBE**	47	-2.00096	-0.70818	0.00031	-0.83292
EGBIN	**BENIN**	48	6.44575	-1.89324	0.03866	-0.71487
BENIN	**ASABA**	49	4.4771	-8.64876	0.01594	-10.10761
ASABA	**ONITSHA**	50	4.31116	1.38285	0.01013	-1.12876
IKOT EKPENE	**ODUKPANI**	51	1.14471	-1.97431	0.0017	-1.02356
AIYEDE	**OSHOBO**	52	0.68392	0.03693	0.00019	0.00165
UGWUAJI	**IKOT EKPENE**	53	-2.50418	-4.56154	0.0067	-0.96278
ALAOJI	**IKOT EKPENE**	54	5.47927	1.29084	0.00368	-1.00361
ODUKPANI	**ADIABOR**	55	1.82301	-0.36584	0.00301	-1.03584
Ganmo	**JEBBA**	56	-0.98277	-0.57019	0.00116	0.00995
OSHOBO	**IKEJA W**	57	-4.34481	0.74016	0.00959	0.06677
JEBBA	**OSHOBO**	58	0.08439	0.08293	0.00001	0.00067
TOTAL POWER LOSS					**0.5182**	**-45.34855**

From Table 1 and Figure 3, it can be observed that five buses (Maiduguri, Yola, Gombe, Jalingo and Adamawa) fell below the IEEE acceptable range of 0.95pu to 1.05pu for healthy buses. This result suggests that the system was not stable as power network stability requires that all buses maintain a voltage level within the above stated IEEE acceptable range. Table 2 revealed that the test network recorded a total network real power line loss of **0.5182pu.** To reduce this network line loss and enhance voltage profile and stability, there is need to improve the network Available Transfer Capability (ATC). To enhance the network ATC for an improved voltage profile and reduced line losses, this study proposes the connection of Interline Power Flow Controllers (IPFC) at vulnerable buses. To be able to evaluate the impact of the chosen technique on the enhancement of the test network ATC, there is need to compute the network's ATC before applying the proposed technique on the network.

Vol. 3, No. 6 | 2022 | pp. 38-50 | DOI: https://doi.org/10.5281/zenodo.7433486

Result of Continuations Load Flow

Table 3: Voltage magnitude and angle, active and reactive power at buses after load flow

Bus	***V (pu)***	***phase (pu)***	***P gen (pu)***	***Q gen (pu)***	***P load (pu)***	***Q load (pu)***
ALAOJI	0.99167	-0.14851	0	0	3	-0.69
SAPELLE	1	-0.06141	4	-4.2388	0	0
AKANGBA	0.99503	-0.01663	0	0	2.04	0.95
LEKKI	1.00382	-0.01105	0	0	1.2	0.62
SAKETE	0.99029	-0.03103	0	0	2.04	0.95
AJA	1.00167	-0.00156	0	0	1.2	0.62
JEBBA	1	-0.01493	5.16563	0.58415	0	0
KADUNA	0.89826	-0.16527	0	0	2	0.97
New Haven	0.97	-0.13665	0	0	1.13	0.56
OKEARO TS	0.99719	-0.00952	0	0	2.04	0.95
SHIRORO	1	-0.08805	4.38563	18.75357	0	0
UGWUAJI	0.94283	-0.16458	0	0	1.6	0.95
ADIABOR	0.99825	-0.16283	0	0	1.82	0.67
AFAM	1	-0.15088	4.5	6.11361	0	0
AIYEDE	0.99614	-0.02973	0	0	1.39	0.69
AJAOKUTA	1.00184	-0.06797	0	0	0.64	0.323
ALADJA	0.99979	-0.06425	0	0	1.82	0.67
ASABA	1.00794	-0.08472	0	0	0.15	0.076
BENIN	1.00444	-0.06656	0	0	1.57	0.8
DAMATURU	0.5493	-0.48695	0	0	3.38563	2.18922
DELTA1	1	-0.06332	2.5	-2.39185	0	0
EGBIN	1	0	27.7051	-5.41178	0	0
GEREGU	1	-0.06189	2	-0.82919	0	0
GOMBE	0.5519	-0.48032	0	0	3.98563	2.73922
GWAGWA	0.99979	-0.08688	0	0	2.03	1.02
Ganmo	0.99449	-0.02867	0	0	1.39	0.69
IHOVBO	1	-0.03319	4.38563	-5.3538	0.15	0.076
IKEJA W	0.99564	-0.01564	0	0	4.29	2.48
IKOT EKPENE	0.98238	-0.15506	0	0	1.82	0.67
JALINGO	0.49447	-0.57026	0	0	3.38563	2.08922
JEBBA TS	0.99973	-0.01534	0	0	0.15	0.076
JOS	0.81009	-0.23117	0	0	2.5	1.25
KAINJI	1	0.00233	8.16563	-0.15767	0	0
KANO	0.89007	-0.1794	0	0	2	0.97
KANTANPE	0.99862	-0.08772	0	0	2.03	1.02
KEBBI	0.99846	-0.00106	0	0	1.2	0.4
LOKOJA	1.00129	-0.07766	0	0	0.15	0.076
MAIDUGURI	0.54462	-0.50627	0	0	1	0.3
MAKURDI	0.86331	-0.20318	0	0	1.8	0.65
ODUKPANI	1	-0.16169	2.5	5.12236	1.82	0.67
OKO OBA	1.00029	-0.00303	0	0	1.82	0.67
OKPAI	1	-0.10302	2.5	1.48667	0	0
OLORUNSOGO	1	-0.01347	2.5	-0.23669	0	0
ONITSHA	0.99493	-0.10991	0	0	1.15	0.42
OSHOBO	0.99563	-0.03238	0	0	2.01	1.37
OWERRI	0.98628	-0.16402	0	0	2.04	0.95
YOLA	0.50921	-0.53347	0	0	3.38563	5.78922

Vol. 3, No. 6 | 2022 | pp. 38-50 | DOI: https://doi.org/10.5281/zenodo.7433486

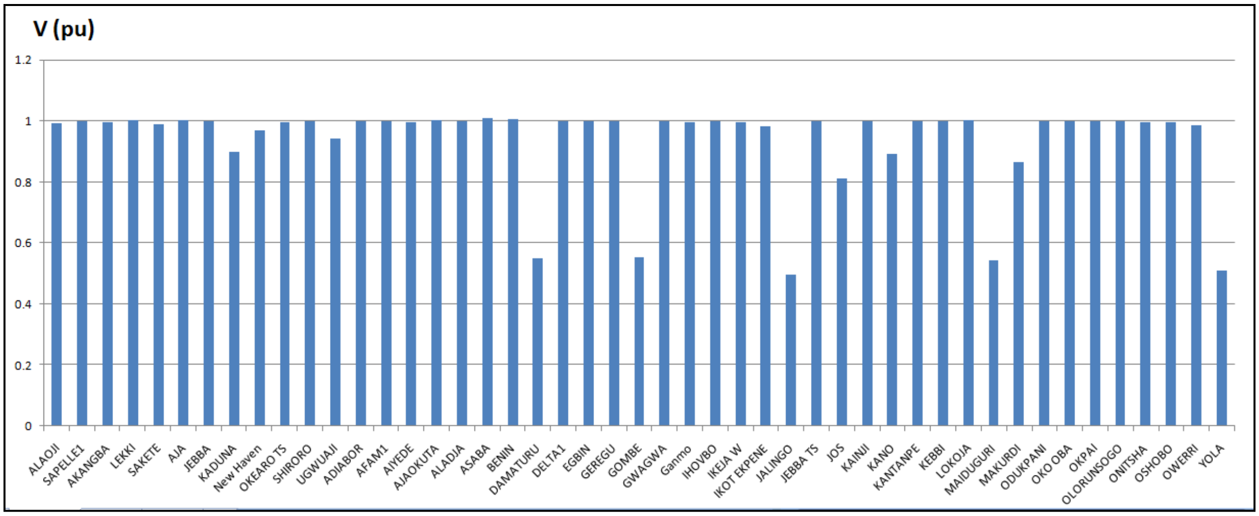

Figure 4: Bar Chart showing voltage magnitude of Test network buses after Continuation Load Flow

Figure 4 and Table 3 present the result of the continuation power flow on the test network. The primary reason for the continuation power flow studies is to obtain the data needed to compute the ATC of the test network. As explained earlier, some selected buses need to be grouped into two areas: source area and Sink area. The source area will be made up of generator buses while the sink area will be made up of load buses. Four generator buses: Kainji, Jebba, Shiroro and Ihovbo are identified as generators in the sources area. Similarly, Yola, Damaturu, Jalingo and Gombe are identified as loads in the sink area. Applying equation 3.15, the network base ATC is computed thus:

$$\mathrm{ATC} = \sum_{i \in sink} \mathrm{P}_{\mathrm{L}}^{i}\,(\lambda_{\max}) - \sum_{i \in sink} \mathrm{P}_{\mathrm{L}}^{io}$$

Sum of P_L^i = 1 +1.6 + 1 +1 =**4.6pu**

Sum of P_L^{i0} = 3.38563 + 3.98563 + 3.38563 + 3.38563 = **13.54pu**

Where$P_L^{i0}$and $P_L^i$are respectively the network real power load after load flow and continuation load flow for the selected buses in the load area.

ATC = 13.54 – 4.6 = 8**.94pu**

Summary and Conclusion

This research work targeted the characterization and modeling of the Nigeria 47 bus 330kVA transmission line network. The findings in this research work showed that the computed ATC of the test network before compensation was found to be 8.94pu. Also, with help of load flow studies, five buses were found to be weak (with a voltage profile less than 0.95pu) while the total network real power loss before compensation was found to be 0.5182pu.

It can be concluded that with the help of load flow and continuation load flow, the Nigeria 330kV power transmission grid network can be characterized to determine parameters/variables of interest including network ATC, power losses, and voltage profiles. A digital model of the test network can also be developed in the PSAT Simulink platform running on Matlab. It is recommended that a suitable FACTS device be optimally sized and placed in the test network to enhance the variables of interest.

Vol. 3, No. 6 | 2022 | pp. 38-50 | *DOI: https://doi.org/10.5281/zenodo.7433486*

References

Ahmad, A. S., Mark, N. N., and Agbachi E. O (2014). Available Transfer Capability ATC a Index for Transmission Network Performance – A Case Study of Nigerian 0kV Tran mi i n Grid. *International Journal on Electrical Engineering and Informatics* 6(3), 479-486.

Chandrasekar, K. and Rsmana N. V. (2011). A fast computational techniques to Assess total transfer capability using brodon- Shamanski. *Global J. f Researches in Engineering*, 11(5), 13 – 15, 2011.

Elias, S. & Sarwary, G. (2017). Importance of Electric Power Transmission Lines for Economy of Afghanistan.

Fosso, O. (2016). Continuation Power Flow – Applications, Implementation and Experiences. 10.13140/RG.2.2.28752.30720.

Gupta J. B. (2014). A course in Power Systems. New Delhi: Sc Chand publishers

Hojabri, M. & Hizam, H. (2011). Available Transfer Capability Calculation. 10.5772/21163.

Mohammed, O. O., Otuoze, A. O., Salisu, S., Abioye, A. E., Usman A. M., & Alao, R. A. (2020). The challenges and panaceas to power distribution losses in Nigeria. *Arid Zone Journal of Engineering, Technology & Environment* 16(1): 120-136

Naresk, Y. and Prashant, S. (2013). Available transfer capability using DCPTDF incorporating multiple line contingences and generator addition under deregulated environment. *Int. J. of Advanced Research in Electrical, Electronics and Instrumentation Engineering*, 2(6), 2297 – 2300

Natália M. R., Santo, O. P., Dia, V. & Fernão, P. (2018). Determination of available transfer capability (ATC) in a competitive electricity market using Nigerian 3-bus and 14-bus power network as case study. *Nigerian Journal of Technology (NIJOTECH),* 37(3), 786 – 794

NERC Report, June 1996 NERC, *Available Transfer Capability Definitions and Determination.*

Nigerian Power sector review report, December 2009, African Development.

Rachmawatie, D., Rustiadi, E., Fauzi, A., & Juanda, B. (2019). Analysis of the socio-economic impact of renewable energy hybrid electricity utilization for rural community development (case study: Pantai Anyar, Yogyakarta special region, Indonesia). IOP Conference Series: Earth and Environmental Science 383. 012013. 10.1088/1755-1315/383/1/012013.